2003

The effect of turbulence on forced convection from a heated horizontal circular cylinder.

Christopher. Sak
University of Windsor

The Effect of Turbulence on Forced Convection from a Heated Horizontal Circular Cylinder

by
Christopher Sak

A Thesis
Submitted to the Faculty of Graduate Studies and Research
through the Department of Mechanical, Automotive & Materials Engineering
in Partial Fulfillment of the Requirements for
the Degree of Master of Applied Science at the
University of Windsor

Windsor, Ontario, Canada
2002

Your file Votre référence
ISBN: 0-612-84546-X
Our file Notre référence
ISBN: 0-612-84546-X

975441

ABSTRACT

The effects of free stream turbulence integral length scale and turbulence intensity (root-mean-square stream-wise component of velocity fluctuation) on the rate of forced convective heat transfer from a heated horizontal circular cylinder in a cross flow of air were investigated experimentally. An internally heated 5.1 cm (2") diameter aluminium cylinder was placed horizontally in an 86 cm wide by 66 cm high (34" by 26") wind tunnel. The power supplied by the internally embedded heater was kept constant in order to maintain uniform surface temperature. A perforated plate was placed at the entrance to the test section to generate the free stream turbulence. To eliminate the effect of the mean free stream velocity, the Reynolds number based on the cylinder diameter was kept at 27,700 ± 1850. By altering the solidity area ratio, the diameter of the perforated holes and/or the distance downstream of the plate the turbulence integral length scale ratio, L/D, where D is the diameter of the cylinder and the turbulence intensity, Tu, were varied independently. The turbulence integral length scale was varied from 0.50 to 1.47 with turbulence intensity fixed at 6.7% ± 0.3% in one experiment while the turbulence intensity was altered from 3.0 to 8.2% with turbulence length scale ratio fixed at 0.78 ± 0.03 in another. The free stream turbulence parameters measured in the absence of the cylinder were correlated with the temporal and spatial (mean of the entire cylinder) averaged convective heat transfer coefficient. A comparison with the case of no turbulence generation was also made. In this case the Reynolds number was changed over the range $18{,}000 < Re < 34{,}000$.

Over the range of conditions considered, the data shows that increasing the mean free stream Reynolds number resulted in an increase in the heat transfer rate from the cylinder. For the case of fixed turbulence length scale, an increase in turbulence intensity resulted in an increase in heat transfer whereas for the case of fixed turbulence intensity, an increase in turbulence length scale resulted in a decrease in heat transfer.

To those who matter most.

ACKNOWLEDGEMENTS

The author wishes to express his forthright gratitude to Dr. D.S-K. Ting and Dr. G.W. Rankin for their relentless guidance and unremitting support throughout the duration of the research. Without their sincere honesty and invaluable wisdom this work would not have been completed with the same zeal and fervour demonstrated and carried out by the author.

The secretarial assistance provided by Ms. R. Gignac is also greatly valued and acknowledged. The assistance of Mr. P. Seguin in regards to technical and electronic issues is duly appreciated. Additional thanks are extended to the University of Windsor Technical Support Centre, especially Mr. M. St. Pierre and Mr. S. Budinsky, for the construction of the cylinder and supporting apparatus.

Financial support from the Natural Sciences and Engineering Research Council of Canada (NSERC) through their Discovery and Equipment Grant Programs is gratefully recognized. Additionally, thanks are extended to the Department of Mechanical, Automotive & Materials Engineering at the University of Windsor for their financial support through a Graduate Assistantship award.

TABLE OF CONTENTS

LIST OF TABLES

LIST OF FIGURES

NOMENCLATURE

A_s	surface area of cylinder [m^2]
Bi	Biot number, hL_c/k_{Al}
c_p	specific heat [J kg^{-1} K^{-1}]
D	cylinder diameter [m]
e	instrument error
Fr	Frossling number, $Nu/Re^{1/2}$
h	heat transfer coefficient [W m^{-2} K^{-1}]
g	acceleration due to gravity, 9.81 m s^{-2}
k_{air}	thermal conductivity of air [W m^{-1} K^{-1}]
k_{Al}	thermal conductivity of aluminium [W m^{-1} K^{-1}]
L	turbulence integral length scale [m]
L_c	characteristic length of the circular cylinder [m]
ℓ	length of the test heater [m]
ℓ_{oil}	amount of oil in manometer [m]
N	total number of measurements
Nu	Nusselt number, hD/k_{air}
P	barometric pressure [Pa]
Pr	Prandtl number, $\mu c_p/k_{air}$
Q_{cond}	energy transfer due to conduction [W]
Q_{conv}	energy transfer due to convection [W]
Q_{rad}	energy transfer due to radiation [W]
Q_{tot}	total power [W]
R	universal gas constant, 287.0 J kg^{-1} K^{-1}
Re	Reynolds number, $\overline{U}D/\nu$
S	standard deviation
$\langle S \rangle$	pooled standard deviation
$\mathcal{S}$	solidity area ratio of perforated plate, solid area/total area of plate [%]

T_f film temperature, $\frac{1}{2}(T_s + T_\infty)$ [°C]

T_r initial room temperature [°C]

T_s surface temperature of cylinder [°C]

T_∞ free stream temperature [°C]

t time [s]

$t_{N\text{-}1,95}$ t variable at 95% probability

Tu turbulence intensity, $u'/\overline{U}$ [%]

U velocity of a turbulent flow, $\overline{U} + u$ [m s^{-1}]

$\overline{U}$ mean velocity [m s^{-1}]

u fluctuation of velocity [m s^{-1}]

u' root-mean-square of the velocity fluctuations [m s^{-1}]

V volume of cylinder [m^3]

w overall uncertainty

w_c instrument calibration uncertainty

w_0 zero-order uncertainty

w_1 first-order uncertainty

w_2 second-order uncertainty

X distance downstream from the perforated plate [m]

Greek Symbols

ε emissivity

θ angle measured from the front stagnation point of circular cylinder [°]

μ dynamic viscosity of air [kg m^{-1} s^{-1}]

ν kinematic viscosity of air, μ/ρ_{air} [m^2 s^{-1}]

ρ_{air} density of air [kg m^{-3}]

ρ_{H_2O} density of water [kg m^{-3}]

σ Stefan-Boltzmann constant, 5.67 x 10^{-8} W m^{-2} K^{-4}

τ_Λ integral time scale [s]

ϕ hole diameter of the perforated plate [m]

CHAPTER 1 – INTRODUCTION

1.1 Significance and Subject of Investigation

Bluff bodies in a cross flow are common elements found in many practical applications. They include circular cylinders (as is the case for the current research), rectangular or elliptic pipes, or bodies of other geometry. Circular cylinders, however, find perhaps the most widespread application in heat exchangers, power generators, and other thermal equipment. Circular cylinders or tubes of other cross sectional shapes are also used in buildings; for example, pipelines, chimneys, poles, supports, columns, etc. It is therefore of great importance to gain a better understanding of the effect that free stream turbulence has on the heat transfer rate from bluff bodies.

Many experimental investigations involving bluff bodies in a cross flow have shown that the convective heat transfer from a bluff body is dependent upon numerous factors such as material type, size of the body, temperature difference between body and flow, Reynolds number, Prandtl number, blockage effect, surface roughness of the body and the spatial flow structure in the wake [1, 2]. Another factor that is equally important is that of free stream turbulence. Turbulence and the effect it has on the heat transfer rate, most notably, the way it augments heat transfer in forced convection is an important, and hence, greatly researched area. There are many studies involving the effect of turbulent flow on the heat transfer rate from a bluff body, but very few investigate the Nusselt number variation with respect to, Reynolds number, turbulence intensity and turbulence length scale independent of one another.

In the current research, an internally heated circular cylinder of uniform surface temperature was placed horizontally in a wind tunnel and exposed to a turbulent airflow. The surface of the cylinder was cooled at a rate that was ultimately dependent upon the flow parameters, namely, Reynolds number, turbulence intensity, and turbulence length scale. The convective heat transfer coefficient was computed through an analysis that eliminated the effect of losses due to conduction and radiation. Thermocouples, located

on the surface of the cylinder, were used to determine the temperature of the surface, and a thermocouple located in the wind tunnel, yielded the corresponding airflow temperature. Located at the entrance to the wind tunnel was a turbulence-producing perforated plate. Numerous perforated plate configurations were used to control the characteristics of the turbulence produced.

1.2 Objectives

The objectives of this study are to (in a dimensionless manner):

- Develop a relationship between heat transfer from a circular cylinder and mean flow velocity in a controlled environment.
- Determine the effect of turbulence intensity on the heat transfer rate.
- Determine the effect of turbulence integral length scale on the heat transfer rate.
- Make comparisons with other experiments found in the literature.

CHAPTER 2 – LITERATURE REVIEW

2.1 Circular Cylinder in Cross Flow

The flow over a circular cylinder has been the subject of intense scrutiny for a very long time because of its importance in a variety of applications [3, 4]. As illustrated in Figure 2.1, when a circular cylinder is situated in a laminar cross flow, a laminar boundary layer is initially present on the front part of the surface and the fluid flow follows the cylinder contours for very low Reynolds number (Figure 2.1a). As Reynolds number increases, the flow separates from the back of the cylinder and a symmetric pair of vortices form in the wake (Figure 2.1b). As Reynolds number is further increased, the wake becomes unstable and the vortices alternately break away. A laminar periodic wake of staggered vortices of opposite sign (vortex street) is then formed. The vortices breaking away from the cylinder become turbulent, however, the boundary layer on the cylinder remains laminar (Figure 2.1c). The Reynolds number range $150 < Re < 3x10^5$ is called sub-critical. In this range (Figure 2.1d), the vortex street undergoes turbulent transition. Most studies, including the one being presented, fall into the sub-critical range. For the next range, known as the transitional range ($3x10^5 < Re < 3x10^6$), the cylinder boundary layer gradually becomes turbulent and the wake becomes narrower and disorganized (Figure 2.1e). Finally, in the super-critical range ($Re > 3x10^6$), regular turbulent vortex shedding is re-established with a turbulent cylinder boundary layer (Figure 2.1f).

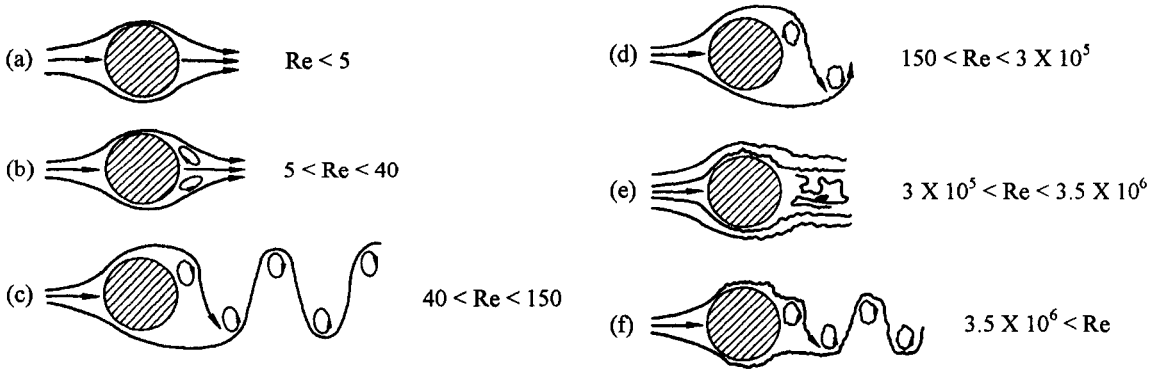

Figure 2.1. Flow over a circular cylinder with varying Reynolds number, from Blevins [3].

All boundary layers begin at the stagnation point and remain laminar for a certain distance downstream, depending on the nature of the flow impinging on the surface. If the prevailing velocity is sufficiently high and the surface sufficiently long then the layer will become turbulent. The characteristic that distinguishes the turbulent from the laminar flow is its ability to transport momentum, and hence, heat laterally. When the boundary layer becomes turbulent the heat transfer rate from the cylinder changes significantly.

2.2 Fluid Flow Effects on Heat Transfer from a Circular Cylinder

Heat transfer from a circular cylinder occurs through three main mechanisms, convection, radiation, and conduction. For the present study, the effects of conduction and radiation were small, thus making the effect due to convection the main mode of heat transfer. It is known that convection heat transfer from a circular cylinder strongly depends upon such fluid properties as dynamic viscosity, thermal conductivity, density and specific heat, and fluid velocity [5]. It also depends on geometrical factors such as size and shape, as well as roughness of the solid surface. In the case of a turbulent free stream, the turbulence intensity and turbulence length scale are also important. A dimensional analysis for the case of heat transfer from a circular cylinder situated in a turbulent airflow, excluding the effects of surface roughness and geometrical shape, yields the following dimensionless variables.

1. Nusselt number, $\mathrm{Nu} = hD/k_{air}$
2. Reynolds number, $\mathrm{Re} = \overline{U}D/\nu$
3. Prandtl number, $\mathrm{Pr} = \mu c_p/k_{air}$
4. Turbulence intensity, $Tu = u'/\overline{U}$
5. Turbulence length scale, $L = \overline{U} \cdot \tau_\Lambda$

These last four factors (Re, Pr, Tu, and L) then become the parameters that affect the heat transfer problem (characterized by Nu). The complicated flow pattern that occurs around

a circular cylinder (Figure 2.1) is known to greatly influence heat transfer and has been studied experimentally by numerous researchers. For example, Churchill and Bernstein [4] proposed a correlation for convective heat transfer for a circular cylinder in cross flow. The average Nusselt number calculated for Re > 10,000, Re Pr > 0.2 and based on a uniform surface temperature assumption was,

$$\mathrm{Nu} = 0.3 + \frac{0.62\,\mathrm{Re}^{1/2}\,\mathrm{Pr}^{1/3}}{\left[1+(0.4/\mathrm{Pr})^{2/3}\right]^{1/4}}\left[1+\left(\frac{\mathrm{Re}}{282000}\right)^{5/8}\right]^{4/5}. \tag{2.1}$$

Smith and Kuethe [6] found that for a heated circular cylinder in cross flow of air (Pr = 0.7) for a range of Reynolds number from 20,000 to 250,000, the following relation was deduced,

$$\mathrm{Nu} = \sqrt{\mathrm{Re}}\,. \tag{2.2}$$

An empirical approximation given by Çengel [7], which represents the average Nusselt number for forced convection over a circular cylinder for a range of Reynolds number between 4000 and 40,000 and Re Pr > 0.2, was given as,

$$\mathrm{Nu} = 0.193\,\mathrm{Re}^{0.618}\,\mathrm{Pr}^{1/3}. \tag{2.3}$$

2.3 Turbulent Flow

Most flows occurring in engineering applications, especially those dealing with bluff bodies are turbulent. For example, areas where free stream turbulence is encountered includes: heat exchangers, vehicles, turbine engines, rocket nozzles, electronic cooling passages, geophysical flows, and in the chemical, petroleum and food industries, more specifically, areas that involve foods which experience freezing, thawing, reheating and/or drying [8-12]. Since turbulence is associated with the existence of random fluctuations in the fluid, then at least on a short time scale, the flow is inherently

unsteady. Due to this randomness, it is difficult to predict how free stream turbulence affects the heat transfer characteristics of a bluff body.

The important characteristics associated with a free stream turbulent flow are its randomness and wide range of space and time scales. As illustrated in Figure 2.2, the velocity measured at a given point within a steady turbulent flow fluctuates randomly. Thus, the velocity of a turbulent flow, represented by U, can be thought to consist of two main components, the first being a mean velocity, $\overline{U}$, and the second being the velocity fluctuation, u, relative to the mean value.

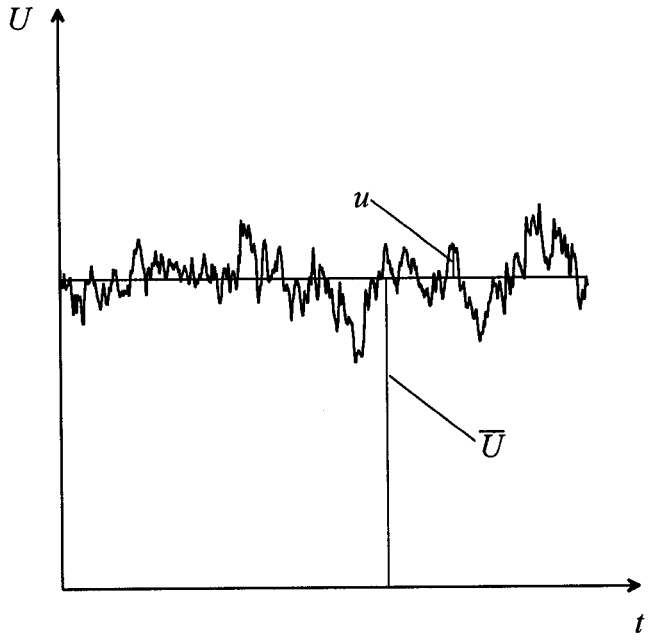

Figure 2.2. Velocity variations with time at some point in a steady turbulent flow.

In general, the Reynolds number, Re, is required to characterize any flow, however, for a turbulent flow, turbulence intensity, Tu, and turbulence length scale, L, are also required. In order to determine an adequate relationship between heat transfer and turbulence, the individual effects of the turbulence length scale and the turbulence intensity, in addition to Reynolds number must be taken into consideration [13].

The turbulence intensity is typically defined as the root-mean-square of the stream-wise component of the velocity fluctuation, u', divided by the mean velocity of the flow,

$\overline{U}$. In most instances it is usually represented as a percentage. In other words, the turbulence intensity represents the strength of the random fluctuations occurring over the duration of the flow (or intensity indicates the amplitude of the fluctuating components of velocity [14]). This relationship can be denoted in the following manner,

$$Tu = \frac{u'}{\overline{U}} \text{ x } 100\%, \tag{2.4}$$

where $u' = \sqrt{\overline{u^2}}$ (u is the velocity fluctuation as illustrated in Figure 2.2).

The turbulence length scale corresponds to a dimension associated with the relative size of the vortices (or eddies) existing in the flow [15]. Turbulence length scale provides an important measure of the distance over which the velocity fluctuations are correlated. A literature review reveals a myriad of length scale definitions, where the most common length scale associated with heat transfer research is the integral scale [16]. In the present research, the length scale of turbulence is normalized by the diameter of the aluminium cylinder, to yield an expression represented as *L/D*, which is known as the turbulence length scale ratio.

2.4 The Role of Turbulence in Heat Transfer

There has been ample research conducted concerning heat transfer rates from bluff bodies exposed to turbulent flow. Research has proven that both the turbulence integral length scale and the turbulence intensity do indeed affect the heat transfer from a circular cylinder and other bluff bodies. Unfortunately, most of the research performed on flow over a bluff body has included measurements using only one of these two turbulence-defining parameters, while allowing the other one to vary without proper control or monitor. A study of the results of various researchers who have considered both the effects of turbulence intensity and turbulence length scale [13, 15, 17-23] yielded inconclusive findings. Most researchers agree that turbulence intensity and turbulence length scale play critical roles in determining the rate of heat transfer from circular cylinders in cross flow. The extent of this role remains unclear.

2.4.1 Turbulence Intensity Effects on Heat Transfer

The prevailing notion among researchers is that as free stream turbulence intensity increases, the heat transfer rate also experiences an increase [8-10, 13]. This is known to be true for comparisons made between an average heat transfer coefficient determined around a circular cylinder and a turbulent airflow for the condition of uniform surface temperature. It has been proposed that increases in turbulence intensities produce higher heat transfer coefficients through: a direct increase in heat transfer to the laminar boundary layer, an earlier transition to turbulence, and substantial changes in the characteristics of the separated flow [1]. It has also been generalized that turbulence intensity has a more profound effect on the average heat transfer coefficient compared with the turbulence length scale.

Many researchers [8-11, 13, 14, 17-19, 21-23] have studied the influence of turbulence intensity on heat transfer. As illustrated in Figure 2.3 (where turbulence length scale was not held constant), as turbulence intensity increased at a constant Reynolds number, an increase in Nusselt number, Nu, was also experienced. For the three cases shown, the increases in heat transfer with increased turbulence intensity are greater for high rather than for low Reynolds numbers. Nusselt number is very sensitive to small changes in turbulence intensity when turbulence intensity is small (Tu = 0.3% and Tu = 0%), and less sensitive for large turbulence intensity (Tu = 12%). It is also true that Nusselt number is more sensitive to Reynolds number for large compared to small values of constant turbulence intensity.

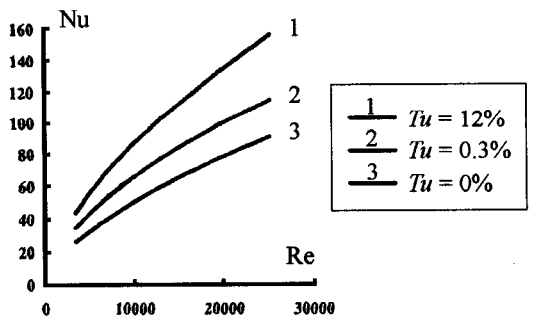

Figure 2.3. Comparison of Nusselt number at different levels of turbulence intensity, modified from Kondjoyan and Daudin [10].

Kondjoyan and Daudin [9] studied the effects of free stream turbulence intensity on heat transfer at the surface of a circular cylinder in cross flow of air (Pr = 0.7) for uniform surface temperature. Without monitoring turbulence length scale effects, an expression relating Nusselt number to turbulence intensity for 3000 < Re < 40,000 and 1% < Tu < 45%, was given as,

$$\mathrm{Nu} = \left(1.07 + 0.015 Tu\sqrt{\mathrm{Re}}\right) 0.63\sqrt{\mathrm{Re}}\,. \tag{2.5}$$

Lowery and Vachon [14] obtained data regarding the effect of free stream turbulence on heat transfer from heated cylinders placed normal to an airflow (Pr = 0.7) for uniform surface temperature. A correlation relating the overall heat transfer to the turbulence intensity for Reynolds number ranging from 109,000 to 302,000, turbulence intensity ranging from 0.4 to 14.2%, and turbulence length scale ratio ranging from 0.015 to 0.095, was given as,

$$\mathrm{Nu} = 0.686\sqrt{\mathrm{Re}} + 0.043 Tu\,\mathrm{Re}\,. \tag{2.6}$$

Sikmanovic et al. [23] deduced a relationship for the case of heat transfer from a circular cylinder in a turbulent airflow (Pr = 0.7) for uniform surface temperature. Measurements were performed at a Reynolds number of 19,000, turbulence intensity ranging from 2.5 to 16% and turbulence length scale ratios ranging from 0.05 to 0.19. Their expression was given as,

$$\mathrm{Nu} = 0.25\,\mathrm{Re}^{0.618} + 0.488\,\mathrm{Re}^{1.118}\left(\frac{Tu}{100}\right) - 0.914\,\mathrm{Re}^{1.618}\left(\frac{Tu}{100}\right)^2. \tag{2.7}$$

Mehendale et al. [11] found a correlation for the overall heat transfer coefficient for Reynolds number ranging from 25,000 to 100,000, along with turbulence intensity ranging from 0.73 to 15.2% for uniform surface temperature at Pr = 0.7. The expression derived was as follows,

$$\mathrm{Nu} = 0.902\sqrt{\mathrm{Re}} + 2.14\,\mathrm{Re}\left(\frac{Tu}{100}\right) - 2.89\sqrt{\mathrm{Re}^3}\left(\frac{Tu}{100}\right)^2. \qquad (2.8)$$

Equations 2.5 to 2.8 all took the general form, $\mathrm{Nu} = a\mathrm{Re}^b + c\mathrm{Re}^d Tu$, thus leading the author to believe that the relationship to be determined for the current study between heat transfer and turbulence intensity will closely resemble this form. It is also important to note that numerous researchers [24-26] studied the effect of turbulence intensity on the local heat transfer rate at the front stagnation point of a circular cylinder in cross flow. All concluded that the Nusselt number increased with increasing turbulence intensity.

2.4.2 Turbulence Length Scale Effects on Heat Transfer

The effects of turbulence length scale on heat transfer can be as important as the effects of turbulence intensity. It has been suggested that as free stream turbulence length scale increases, the overall heat transfer rate decreases [27]. Sunden [21] suggested that for constant turbulence intensity, the heat transfer coefficient increased in the range $0 < L/D < 1.6$ but decreased when $L/D > 1.6$, thus experiencing a peak at $L/D = 1.6$. Similarly, Van der Hegge Zijnen [13] found that a maximum increase in heat transfer occurred at $L/D = 1.6$ for a turbulence intensity between 2 and 13% and Reynolds number between 2000 and 25,800. In Yardi and Sukhatme's [22] experiment for Reynolds number ranging from 6000 to 100,000 and turbulence intensity ranging from 0.2 to 7.0%, it was also found that the influences of turbulence length scale on heat transfer led to a maximum or peak. This was confirmed by Zukauskas et al. [19], but in their experiment, the Reynolds number ranged from 10^4 to 10^6 at constant turbulence intensity (Tu = 0.5%), where this maximum occurred at $(L/D)\,\mathrm{Re}^{1/2} = 10$. This is illustrated in Figure 2.4, where after an initial increase, the K value (where $K = \mathrm{Nu}/\mathrm{Re}^{1/2}\,\mathrm{Pr}^{1/3}$) reaches a maximum, at which point a steady decrease occurs as the turbulence length scale ratio increases. Substituting $\mathrm{Re} = 10^4$, would yield $L/D = 0.1$, which is well below the turbulence length scale ratio for a maximum heat transfer rate proposed by Sunden ($L/D = 1.6$).

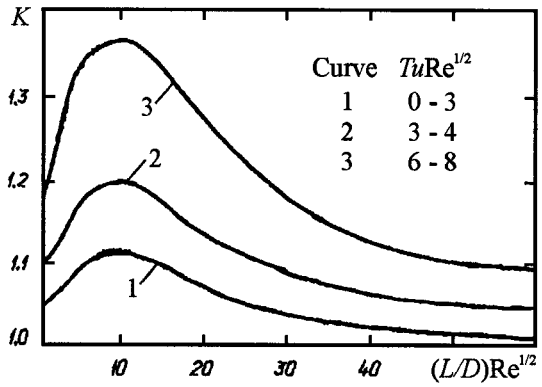

Figure 2.4. The effect of turbulence length scale on heat transfer, modified from Zukauskas et al. [19].

Sunden [21] also claimed that the effect of turbulence length scale is almost imperceptible at low turbulence intensity values (approximately 1.25%), but becomes significant at Tu = 6.13%. A plot of Frossling number, Fr (= $Nu/Re^{1/2}$), versus the turbulence length scale ratio is illustrated in Figure 2.5. It can be seen that at higher turbulence intensities, a more pronounced relationship develops as the turbulence length scale ratio increases.

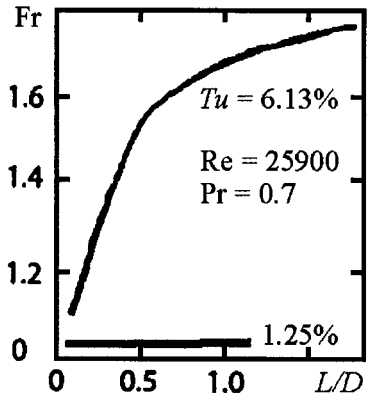

Figure 2.5. Frossling number versus turbulence length scale, from Sunden [21].

Torii and Yang [27] studied the effects of turbulence length scale on heat transfer. For a circular cylinder positioned normal to an airflow (Pr = 0.7) for a Reynolds number ranging from 7000 to 13,000, turbulence length scale ratio ranging from 0.79 to 1.78, and Tu < 1.0% (turbulence can be considered negligible), an expression relating Nusselt number with turbulence length scale was found to be,

$$\mathrm{Nu} = 0.15\,\mathrm{Re}^{2/3}(L/D)^{-0.66}. \tag{2.9}$$

The question that ultimately remains unresolved in the literature is the role that the two turbulent flow parameters (turbulence length scale and turbulence intensity) have on the heat transfer rate independent of one another. Differentiating turbulence length scale effects from turbulence intensity effects will allow a more accurate and methodical approach in determining the effect that each of these parameters has on the overall heat transfer rate.

CHAPTER 3 – EXPERIMENTAL DETAILS

3.1 Wind Tunnel

The experiments were conducted in a wind tunnel with a test section measuring 86 cm wide by 66 cm high by 238 cm long (34" by 26" by 94") as shown in Figure 3.1. The wind tunnel consisted of four panels where the top and the two side panels were made of acrylic and the bottom panel was made of 1.6 cm (⅝") thick plywood. Four brackets were used to secure the top panel to reduce the vibration caused by the blower and/or the flowing air. In the absence of turbulence producing perforated plates (where *Tu* was no larger than 0.6%), the blower was capable of producing varying levels of free stream velocity ranging from approximately 4 to 20 m/s. Slots were cut into the base panel of the wind tunnel in order to reduce the length of the heater lead wires and thermocouple wires which were connected to the data acquisition equipment. These slots, when not in use, were covered with tape in order to prevent any changes in boundary layer due to flow restrictions.

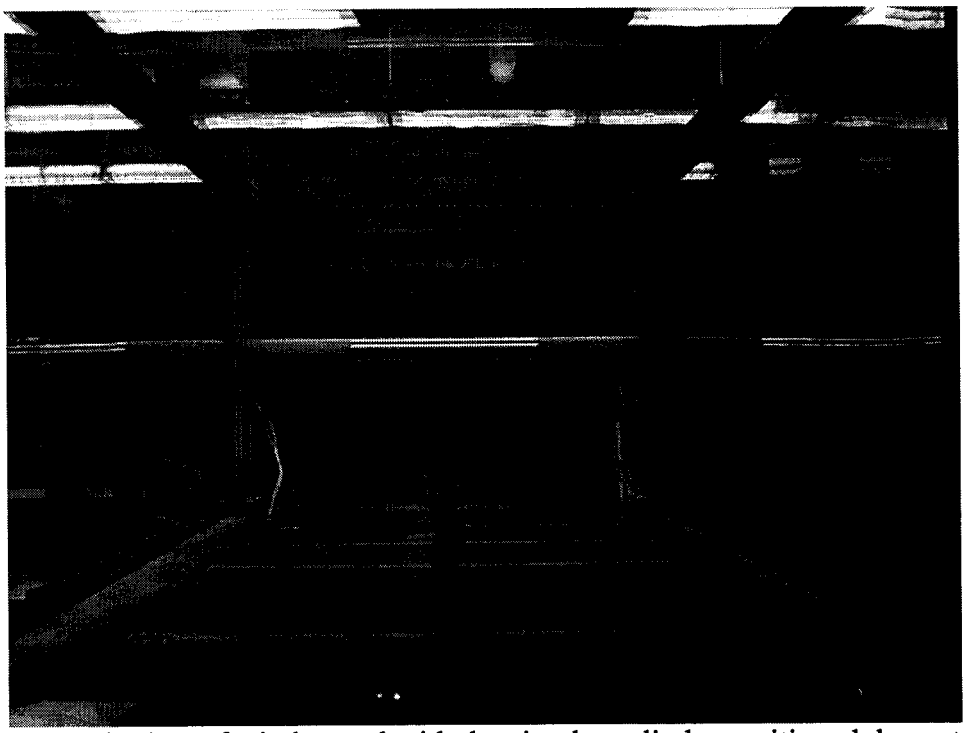

Figure 3.1. Exit view of wind tunnel with the circular cylinder positioned downstream of the turbulence generating perforated plate.

3.2 Turbulence Generation

In order to generate turbulence of the desired intensity and integral length scale, 3 mm thick aluminium sheet metal perforated plates were used. An example of a perforated plate used is shown in Figure 3.2. Perforated plates were chosen to generate a flow that approximated homogeneous and isotropic turbulence based upon a previous experimental study [28]. These perforated plates were attached at the entrance of the test section and consisted of various hole diameters, ϕ, and solidity area ratios, $\mathcal{S}$. The variation of these two parameters along with different levels of free stream mean velocity, $\overline{U}$ led to the attainment of different combinations of turbulence length scales and turbulence intensities at different downstream locations. Table 3.1 shows the various plate combinations that were available for use in the current experiment. Each plate incorporated one of three hole diameters along with one of three different solidity area ratios, thus allowing for nine different hole - solidity area ratio combinations. The three sizes of hole diameters were arbitrarily chosen. The solidity area ratios were chosen based on specific design requirements that were predetermined in order to obtain nearly isotropic turbulence. De Silva and Fernando [29] established that turbulence producing grids should have a solidity area ratio of no larger than 60% in order to obtain nearly isotropic turbulence. These various plate dimension combinations generated a reasonable range in turbulence intensity and turbulence length scale values that were needed in order to develop a comprehensive set of results.

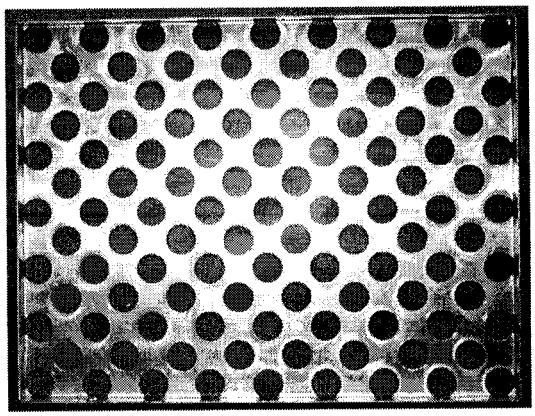

Figure 3.2. Photograph of a turbulence generating perforated plate (Plate #9, ϕ = 5.1 cm, $\mathcal{S}$= 60%).

Table 3.1. Perforated plate characteristics.

Plate	ϕ (cm)	S(%)
1	2.5	35
2	3.8	35
3	5.1	35
4	2.5	50
5	3.8	50
6	5.1	50
7	2.5	60
8	3.8	60
9	5.1	60

3.3 Circular Cylinder

The circular cylinder (Figure 3.3) consisted of three separate sections, where the total length was the same as the width of the wind tunnel, which was approximately 86 cm (34"). The two end sections served primarily as insulators, measuring 23.2 cm (9⅛") in length and 5.1 cm (2") in diameter and were made of Nylon 101. The middle of the three sections consisted of the aluminium cylinder, which had an outer diameter of 5.1 cm (2") and an inner diameter of 1.6 cm (⅝"). The aluminium was type 6061 and polished in order to eliminate any surface roughness effects. Three independently controlled, 12.7 cm (5") long cartridge heaters were embedded in the centre of the aluminium cylinder in order to provide the necessary heat to the cylinder wall. The cylinder was mounted horizontally with its axis perpendicular to the flow at a position halfway between the roof and the floor of the wind tunnel. Each end of the cylinder was inserted into a 1.3 cm (½") thick wooden stand (see Figure 3.1). These stands allowed for longitudinal movement along the length of the wind tunnel, which in turn, allowed the distance downstream from the perforated plate, X, to be altered accordingly. In this way the cylinder was positioned at specific downstream points where certain turbulence intensities and turbulence length scales existed. In addition, the blockage was relatively low at approximately 7.7% and its effects were neglected.

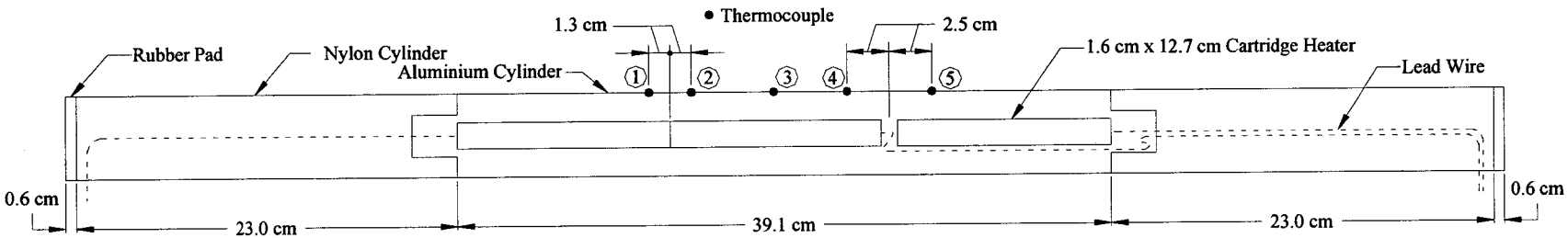

Figure 3.3. Schematic of the circular cylinder used.

3.4 Heaters

The heaters used in this study were 625W OMEGA cartridge heaters that were 1.6 cm (⅝") in diameter and 12.7 cm (5") long. They had 16-gage stranded copper lead wire to allow connection to the power source. An illustration of the cartridge heater is shown in Figure 3.4. The cartridge heaters were constructed of high-temperature Incoloy sheath material. A nickel-chromium resistance wire was used for the resistance winding which was densely compacted to improve its thermal conductivity and dielectric strength. It was determined that a 625W heater was sufficient for this study considering that a maximum temperature of approximately 40°C above room temperature was to be implemented. The two outer heaters served as guard heaters, which were regulated to provide uniform surface temperature along the length of the aluminium cylinder. This eliminated axial conduction loss and forced all heat transfer to occur in the radial direction.

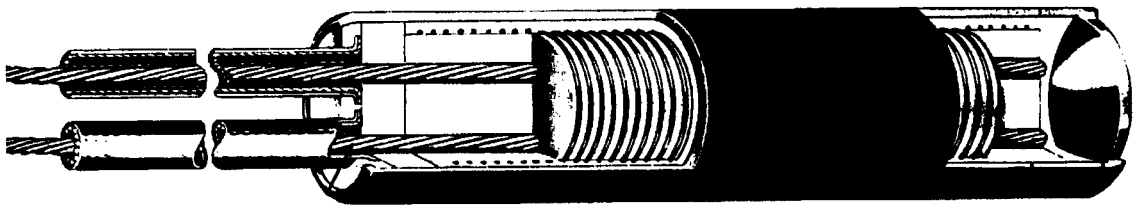

Figure 3.4. Picture of the cartridge heater embedded in circular cylinder, from Omega Engineering [30].

3.5 Thermocouple Arrangement

The aluminium cylinder incorporated five thermocouples that were placed along the circumference of the cylinder. A small slot was cut into the surface of the cylinder in order to embed the thermocouple wires, thus avoiding any flow disturbances caused by having the wires exposed to the airflow. The slot was filled with Plastic Steel® Putty (A), an epoxy metal which has properties that closely resemble those of aluminium. Thermocouples 1, 2, 4 and 5 (Figure 3.3) were placed symmetrically on either side of the gap that was associated with each adjoining cartridge heater in order to check the axial temperature gradient. Thermocouple 3 was located directly in the middle of the cylinder

and was designated as the 'test' thermocouple. The reading provided by this thermocouple was used to determine the overall average heat transfer coefficient, h. For the purpose of this experiment, Type T thermocouples were selected, as they are very sensitive and are accurate in the range of 20 to 70°C (see Appendix A for a complete analysis of all thermocouples considered).

3.6 Cylinder Design

A uniform temperature distribution along the length of the cylinder was desired. The Biot number, Bi, plays a fundamental role in conduction problems that involve surface convection effects, as is the case for the current study where the conduction through the aluminium cylinder was affected by the surface convection caused by the turbulent flow. The Biot number provides a measure of the temperature drop in the solid relative to the temperature difference between the surface and the fluid. It is the ratio of the internal resistance of a body to heat conduction to its external resistance to heat convection. The Biot number can be expressed as,

$$\mathrm{Bi} = \frac{hL_c}{k_{Al}}, \tag{3.1}$$

where L_c represents the characteristic length, which is defined as the ratio of the solid's volume to surface area, $L_c = V/A_s$ (= 1.3 cm). Hence, because of the relationship relating the convection at the surface of a body to the conduction within the body, a small Biot number represents a small resistance to heat conduction, and thus small temperature gradients within the body. It has been suggested that for a Biot number much less than 1, it is reasonable to assume a uniform temperature distribution across a solid at any time [5]. For the current study, the Biot number was approximately equal to 0.01, which is sufficiently small, and thus a uniform temperature distribution over the circular cylinder surface is expected. Additionally, a computer simulation using ANSYS confirmed the behaviour of the cartridge heaters in an aluminium cylinder along with the effectiveness of the nylon insulators.

CHAPTER 4 – TURBULENCE AND THERMAL CONDITIONS

4.1 Turbulence Parameter Selection

All turbulence data concerning the flow in the wind tunnel was obtained from a thesis completed by Liu [28]. His results were analysed to identify two distinct sets of data. The first set consisted of constant turbulence length scale with varying turbulence intensity, and the second for constant turbulence intensity with varying turbulence length scale. Fortunately, it was found that for a constant Reynolds number condition, Re = 27,700 ± 1850, there was sufficient data to cover a reasonable range of turbulence intensity and turbulence length scale values. These two sets of data along with the experimental conditions are shown in Table 4.1 and Table 4.2, respectively.

The values in Table 4.1 yielded results that contained approximately similar turbulence length scale ratio, L/D values ranging from 0.73 to 0.82 with an average of 0.78. This means that all of the turbulence length scale ratios are within ± 0.03 or ± 3.9% of each other, which is a reasonable difference considering the scatter in the values that were presented by Liu. Also, the turbulence intensity values cover a range from 3.0 to 8.2% with an uncertainty of 7% of the measured value.

Table 4.1. Flow, perforated plate and cylinder conditions for the case of constant turbulence length scale ratio with varying turbulence intensity.

L/D	Tu (%)	$\overline{U}$ (m/s)	u' (m/s)	Re	ϕ (mm)	$\mathcal{S}$(%)	X (cm)
0.82	3.0	8.5	0.25	26988	50.8	35	203
0.73	3.8	9.0	0.34	28575	25.4	35	76
0.78	4.4	9.0	0.39	28575	25.4	50	102
0.78	7.2	8.5	0.61	26988	50.8	60	102
0.78	7.5	9.0	0.67	28575	25.4	60	51
0.78	8.2	8.6	0.71	27305	38.1	60	76

The values in Table 4.2 contain approximately similar turbulence intensity, *Tu* values ranging from 6.3 to 7.2%, thus yielding an average of 6.7%. This means that all of the turbulence intensities in this range are within ± 0.3 or ± 4.6% of each other. The turbulence length scale ratios cover a range from 0.50 to 1.47 with an uncertainty of 13% of the measured value. Additionally, the root-mean-square stream-wise component of velocity fluctuation was approximately 1.5 times that of the cross-stream value [28].

Table 4.2. Flow, perforated plate and cylinder conditions for the case of constant turbulence intensity with varying turbulence length scale ratio.

Tu (%)	L/D	$\overline{U}$ (m/s)	u' (m/s)	Re	ϕ (mm)	$\mathcal{S}$(%)	X (cm)
6.7	0.50	8.6	0.57	27305	38.1	50	76
6.5	0.70	9.0	0.59	28575	25.4	60	76
6.3	1.04	9.0	0.57	28575	25.4	60	102
6.9	1.05	8.6	0.60	27305	38.1	60	114
6.9	1.19	8.5	0.59	26988	50.8	50	102
7.2	1.47	8.6	0.61	27305	38.1	60	152

4.2 Surface Temperature and Temperature Difference Effects

Preliminary tests were conducted to determine the constancy of the difference between the free stream temperature and that of the circular cylinder surface around its circumference. This was accomplished by performing multiple tests using identical test conditions where the only change was that of rotating the circular cylinder by 30-degree increments. These tests were conducted at two power settings. The results are shown in Figure 4.1, where the temperature difference remained relatively constant for each of the different power settings of the heaters. This indicates that cylinder orientation had negligible effect on the heat transfer rate. It was concluded that whether the thermocouple was located on the downstream facing side of the cylinder or on the upstream facing side of the cylinder, the temperature measurement obtained was approximately similar, thus confirming that a uniform surface temperature condition exists.

Due to the amount of time required for the cylinder to reach steady-state conditions, it was decided for the remainder of the experiments, to keep the power input constant while allowing the temperature difference to vary slightly. This was opposite to keeping the temperature difference constant and varying the power input.

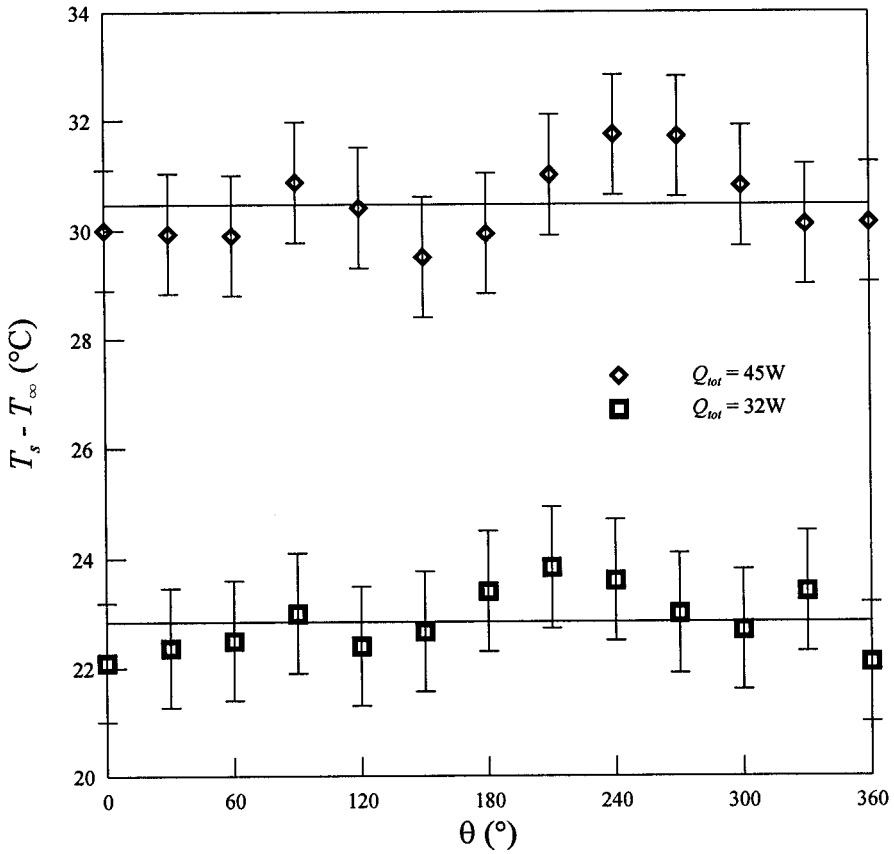

Figure 4.1. Change in temperature around the circumference of the circular cylinder for a change in power input.

CHAPTER 5 – DATA COLLECTION AND PROCESSING

5.1 Fluid Flow Data Collection

For the current study the Reynolds number was defined as,

$$\mathrm{Re} = \frac{\overline{U}D}{\nu}, \tag{5.1}$$

where the mean velocity, $\overline{U}$, was measured using a manometer, the cylinder diameter, D, was measured using a digital vernier, and kinematic viscosity, ν, was determined from tables [7] at standard atmospheric pressure at the film temperature, T_f.

5.2 Turbulence Data Collection

The perforated plate generated turbulent flow was categorized by Liu [28] in terms of mean velocity, $\overline{U}$, turbulence intensity, Tu, and turbulence integral length scale, L. The determination of all turbulent flow data was carried out using a single normal hot-wire probe (DISA type 55P11) and a constant temperature hot-wire anemometer (Dantec Streamline® 55C90 CTA). The hot-wire anemometer calibration was achieved by utilizing a nozzle, Pitot-static tube arrangement. Turbulence statistical quantities such as the turbulence fluctuation velocity, u, the turbulence root-mean-square velocity fluctuations, u', and the integral time scale, τ_Λ (used to calculate the turbulence length scale), were all provided using data analysis programs created by Liu. A sample frequency of 10kHz was used for a sample size of 262,144. The ratio of the turbulence root-mean-square velocity and the mean velocity was used to deduce the turbulence intensity of the flow (equation 2.4), while the turbulence integral length scale was estimated by taking the product of the mean velocity and the integral time scale,

$$L = \overline{U} \cdot \tau_\Lambda . \tag{5.2}$$

Due to the restrictions imposed by the configuration of the hot-wire anemometer, it was not possible to obtain turbulence characteristics at the location where the circular cylinder was positioned. This problem was resolved by adjusting the wind tunnel inlet vane to produce the required mean velocity at a location $10D$ upstream of the circular cylinder. Knowing the mean velocity along with the specific perforated plate used, the corresponding turbulence characteristics at the circular cylinder's location in the absence of the circular cylinder were taken from Liu's results. Additionally, the effect of the turbulence wind tunnel boundary layer was assumed negligible because the test cylinder was positioned at the centre of the wind tunnel far enough away from the walls of the wind tunnel.

5.3 Heat Transfer Data Collection

The overall average heat transfer coefficient, h, due to forced convection was determined by measuring the power input to the internally embedded heater, Q_{tot}, along with calculating the effects due to radiation, Q_{rad}, and conduction, Q_{cond}. Under steady state conditions, the power input was equal to the total heat loss from the cylinder, which in turn, was equal to the heat transferred from the cylinder to the free stream via convection plus radiation and conduction. An energy balance that takes into consideration all the heat supply and heat losses can be written as,

$$Q_{tot} = Q_{conv} + Q_{rad} + Q_{cond}\,. \tag{5.3}$$

Due to the incorporation of guard heaters and end insulators, heat loss due to conduction, Q_{cond}, namely energy loss from the ends of the cylinder was neglected. An overall average convection heat transfer coefficient was calculated based on an average surface temperature. This overall average heat transfer coefficient was assumed to be equivalent for the whole test section of the cylinder because of the approximately constant surface temperature condition over the circumference of the circular cylinder. Thus the heat transfer due to convection can be expressed as,

$$Q_{conv} = hA_s(T_s - T_\infty), \tag{5.4}$$

where T_s is the average surface temperature of the cylinder, ranging from 49 to 63°C from test to test, T_∞ is the free stream temperature taken in the wind tunnel, ranging from 28 to 36°C, and A_s is the surface area of the cylinder over the length of the centre cartridge heater. The circular cylinder also loses heat by radiation to the surrounding air, which can be estimated as,

$$Q_{rad} = \varepsilon\sigma A_s\left(T_s^4 - T_\infty^4\right), \tag{5.5}$$

where ε is the emissivity of the polished aluminium surface, taken to be approximately 0.05 [7] and σ is the Stefan-Boltzmann constant. Substituting equations 5.4 and 5.5 into 5.3 with the condition that $Q_{cond} = 0$ gives,

$$h = \frac{Q_{tot} - \varepsilon\sigma A_s\left(T_s^4 - T_\infty^4\right)}{A_s(T_s - T_\infty)}, \tag{5.6}$$

after rearrangement. Subsequently, the effects of turbulence on heat transfer from the circular cylinder were related by using the dimensionless form of the heat transfer coefficient, i.e., Nusselt number. The Nusselt number is defined as the ratio of convection heat transfer to fluid conduction heat transfer under the same conditions,

$$\mathrm{Nu} = \frac{Q_{conv}}{Q_{cond}} = \frac{hD}{k_{air}}. \tag{5.7}$$

The thermal conductivity of air, k_{air}, was determined at the film temperature.

5.4 Experimental Data Collection

The experimental data consisted of simultaneous measurements of the surface temperature of the circular cylinder and the free stream temperature corresponding to predetermined values of mean flow velocity in the wind tunnel and electrical power dissipation in the 'test' heater. The power input to the 'test' heater was set at a constant value of 32W. The power input to the guard heaters was adjusted so that the guard heaters surface temperature readings (thermocouples 1 and 5, refer to Figure 3.3) were within ± 0.5°C of the 'test' heater surface temperature measurements (thermocouples 2 and 4). This provided the negligible axial conduction condition as discussed in Section 5.3. The pre-test portion of the experiment, common to all data sets, concluded after steady state was attained, typically taking 6-8 hours, and after the initial surface and free stream temperature measurements were recorded.

To determine the relationship between heat transfer and mean flow velocity for the case of negligible turbulence, the velocity of the airflow in the wind tunnel was adjusted in order to obtain Reynolds numbers ranging from 18,000 to 34,000. The mean flow velocity that was required for each specific data set was adjusted by regulating the inlet vane, which was located on the inlet to the blower at the rear of the wind tunnel. Due to the rudimentary construction of the inlet vane, a pressure reading via a manometer was taken in order to confirm the flow setting of the vane was equivalent to the actual flow velocity. The downstream location of the circular cylinder was arbitrarily chosen at X = 114 cm (45"). Also, based on results obtained by Liu [28], the turbulence level present in the absence of the perforated plate was calculated no larger than 0.6%. The surface temperature was obtained in conjunction with the corresponding free stream temperature at 30-degree increments, for one revolution of the circular cylinder. These measurements occurred only after steady state levels were attained, typically taking 15-20 minutes for each 30-degree increment. An average temperature difference was calculated and was used in the determination of the overall average heat transfer coefficient.

In the experiments to determine the relationship between the heat transfer and turbulence intensity, and similarly, between heat transfer and turbulence length scale, the flow, perforated plate and cylinder conditions listed in one of Tables 4.1 or 4.2 were set. The mean flow velocity was set to yield a Reynolds number of 27,700. The perforated plate was attached to the entrance of the wind tunnel, held rigid by six bolts. The downstream location of the circular cylinder varied from 51 to 152 cm dependent upon predetermined conditions. All turbulence related data was obtained as explained in Section 5.2. The measurements of surface (every 30-degrees) and free stream temperature again occurred only after steady state levels were attained. These measurements of temperature were used to determine the heat transfer from the circular cylinder and compared with either turbulence intensity or turbulence length scale.

It is estimated that the various experimental uncertainties associated with the measurements of temperature, power and velocity result in uncertainties not exceeding 6.7% for Reynolds number and 15.3% for Nusselt number (see Appendix B for complete analysis). The uncertainty values associated with turbulence intensity and turbulence length scale were determined by Liu [28] and do not exceed 7% and 13% respectively.

CHAPTER 6 – RESULTS AND DISCUSSION

6.1 Effect of Reynolds Number on Heat Transfer

A relationship between heat transfer and free stream velocity over the circular cylinder is established over the range of Reynolds number considered. Figure 6.1 shows the effect Reynolds number has on the heat transfer rate for the case of low turbulence intensity ($Tu < 0.6\%$). It is expressed in the form of a plot relating Nusselt number versus Reynolds number. It shows that as Reynolds number increases, Nusselt number also increases. Using all experimental data, a correlation equation relating the Nusselt number with Reynolds number over the range $18{,}000 < \mathrm{Re} < 34{,}000$ is obtained as,

$$\mathrm{Nu} = 0.78\sqrt{\mathrm{Re}} - 3.49. \tag{6.1}$$

Studies where similar research was conducted are compared with the current study in Figure 6.1. Churchill and Bernstein [4] claim that equation 2.1 represents the behaviour for the case when low free stream turbulence, negligible blockage, small temperature difference and negligible free convection are present. The values obtained using the correlation proposed by Churchill and Bernstein are lower than the present results. This may be due to the effect of the larger range of Reynolds numbers covered in the current investigation (Churchill and Bernstein included Reynolds numbers as low as 10,000 for their correlation). Equation 2.3 provided by Çengel [7] yields data that is almost identical to that of Churchill and Bernstein and was obtained for $4000 < \mathrm{Re} < 40{,}000$.

The data of Smith and Kuethe [6] using equation 2.2 yields a result that is larger than the current results. Once again, the difference is presumed due to the effect of Reynolds number. Smith and Kuethe covered a range of Reynolds numbers from 20,000 to 250,000, significantly higher than the range used by the author ($18{,}000 < \mathrm{Re} < 34{,}000$) and hence, the correlation is heavily influenced by higher Reynolds number values. Comparing equation 6.1 with the correlation proposed by Smith and Kuethe (equation 2.2) yields a 28% difference in slope.

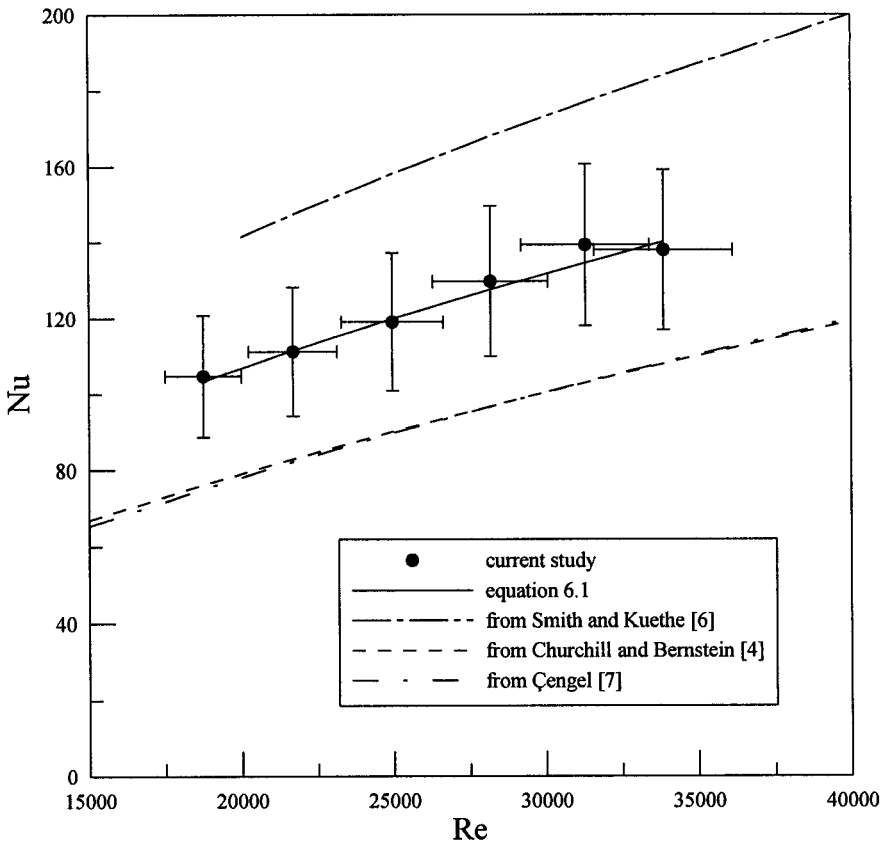

Figure 6.1. Relationship between Nusselt number and Reynolds number for the case of negligible turbulence ($Tu < 0.6\%$).

It should be noted that differences experienced between the current study and other research could also be attributed to various other reasons, such as experimental uncertainty of the data taken from the literature, and different experimental arrangements. These differences notwithstanding, the results show that the Reynolds number is a key contributor to the heat transfer due to forced convection from a bluff body in cross flow. It can be concluded that the effect of increasing Reynolds number leads to an increase in the heat transfer rate.

6.2 Effect of Turbulence Intensity on Heat Transfer

The variation of overall average Nusselt number with changes in turbulence intensity while holding the turbulence length scale and Reynolds number constant is presented in Figure 6.2. The results indicate that, for the range of values considered, increasing the turbulence intensity for a given Reynolds number is associated with an increase in the

overall average Nusselt number at a constant turbulence length scale ratio, L/D = 0.78. This seems reasonable based on previous findings from different researchers which show that an increase in turbulence intensity results in increased heat transfer [8, 10] for high values of Reynolds number (greater than 10^4). For the range of turbulence intensity values considered, a relatively linear relationship seems to exist. It is unclear however, if this trend will continue as the turbulence intensity increases. Also, what is unknown is the effect turbulence length scale has on the relationship between turbulence intensity and heat transfer considering that turbulence length scale is fixed and the author was unable to complete the same comparison for different turbulence length scale values. A correlation equation for the range of data considered was determined as,

$$\mathrm{Nu} = 114.2 + 465.9Tu\,. \tag{6.2}$$

Equation 2.5 proposed by Kondjoyan and Daudin [9] for 3000 < Re < 40,000 and 1% < Tu < 45% yields values that fall slightly below those of the present investigation. Even though the range of Reynolds number and turbulence intensity used in the current investigation fall within the range of values considered by Kondjoyan and Daudin, the discrepancy experienced is presumed to be partly due to the fact that Kondjoyan and Daudin did not monitor turbulence length scale. Also, the arrangement of the experiment somewhat differed as the cylinder used by Kondjoyan and Daudin was made of plaster, not aluminium, and the cylinder had a diameter of 10.0 cm (approximately twice as large as the cylinder used throughout the current study in a wind tunnel that was similar in cross section), thus possibly promoting the blockage effects. Substituting Re = 27,700 into equation 2.5 changes the correlation equation to, $\mathrm{Nu} = 112.2 + 261.8Tu$. This equation is similar to the equation proposed by the author (equation 6.2), where the constant term is almost identical. However, the slope is approximately 78% smaller. This is shown in Figure 6.2 where the relationship between Nusselt number and turbulence intensity is more sensitive for the author's data compared with the data of Kondjoyan and Daudin.

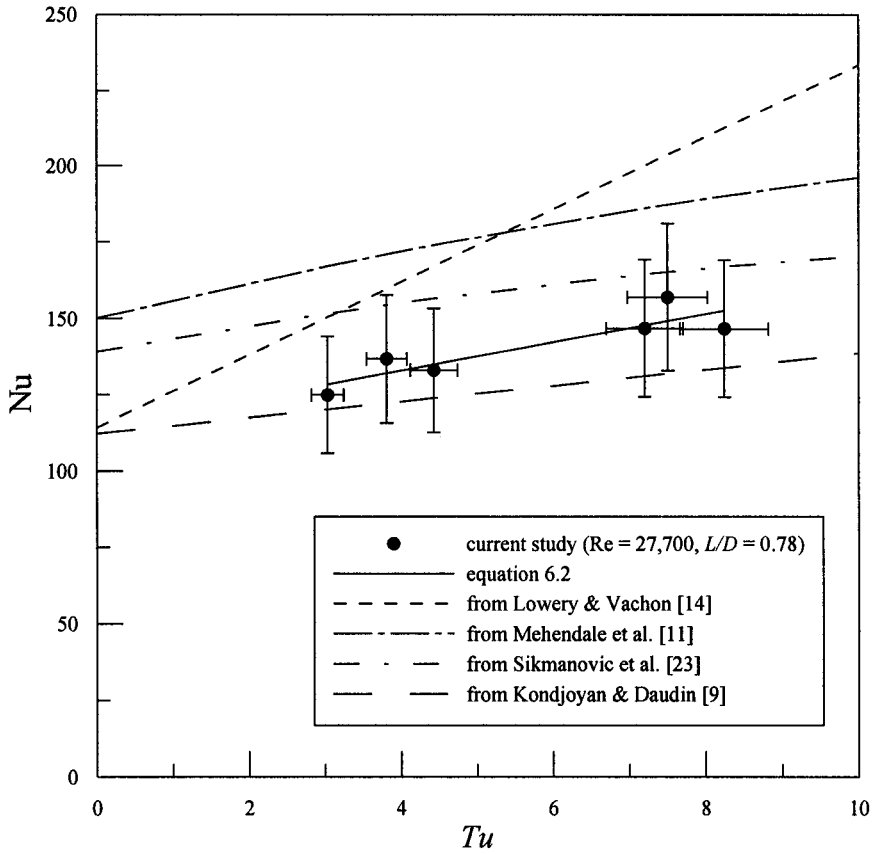

Figure 6.2. Relationship between Nusselt number and turbulence intensity for the case of constant Reynolds number (Re = 27,700) and constant turbulence length scale ratio (L/D = 0.78).

Lowery and Vachon's [14] results, based on equation 2.6, are presented in Figure 6.2. The results yield larger values of Nusselt numbers compared with those obtained by the author. Substituting a Reynolds number of 27,700 into equation 2.6 yields the form, $\mathrm{Nu} = 114.2 + 1191.1Tu$, where it is noticed that the constant term is identical to the current study. The slope of this relation, however, is approximately 2.5 times as large. The difference in the heat transfer rate may be attributed to the fact that Lowery and Vachon performed experiments at a much higher Reynolds number, 109,000 < Re < 302,000. Also they determined the turbulence length scale ratio to be in the range of 0.015 to 0.095, which is significantly lower than the constant turbulence length scale ratio used by the author (L/D = 0.78). Lowery and Vachon [14] concluded that the largest rate of increase in heat transfer with turbulence intensity ($\frac{d\mathrm{Nu}}{dTu}$) occurred approximately at Tu $\mathrm{Re}^{1/2}$ = 10.5. Substituting Re = 27,700, would yield a maximum heat transfer occurring at approximately Tu = 6.3% for the present study. However, it can only be speculated that

this maximum exists for the current study, due to the limited amount of data that was presented and experimental uncertainty.

Sikmanovic et al.'s [23] equation 2.7 yields a pattern similar to that of the current study. The values obtained for Nusselt number were larger over the same range of turbulence intensities. This could be attributed to the difference in experimental conditions, specifically the significantly lower turbulence length scale ratio used throughout the research ($0.05 < L/D < 0.19$). It is presumed that because a smaller turbulence length scale is present, a higher heat transfer rate is experienced.

Mehendale et al.'s [11] relationship yields similar results to that of the work done by Lowery and Vachon. Again a much larger Nusselt number was calculated using equation 2.8 for all values within the range of intensities found in the present study as illustrated in Figure 6.2. These discrepancies could be a result of the Reynolds number being much larger ($25{,}000 < \mathrm{Re} < 100{,}000$) than what was used for the current study and also it was unclear what type of effect turbulence length scale exhibited with regard to heat transfer analysis.

6.3 Effect of Turbulence Length Scale on Heat Transfer

The effect of turbulence length scale on heat transfer with turbulence intensity and Reynolds number held constant is presented in Figure 6.3. It is shown that for constant turbulence intensity and Reynolds number, an increasing length scale ratio results in a decrease in Nusselt number. This suggests that as the length scale grows the enhancement that turbulence has on the heat transfer from the circular cylinder diminishes. This supports previous findings [23, 27] that suggest a negative relationship between Nusselt number and turbulence length scale. A correlation equation is determined for the range of values considered and is given as follows,

$$\mathrm{Nu} = 140.0\left(L/D\right)^{-0.09}. \tag{6.3}$$

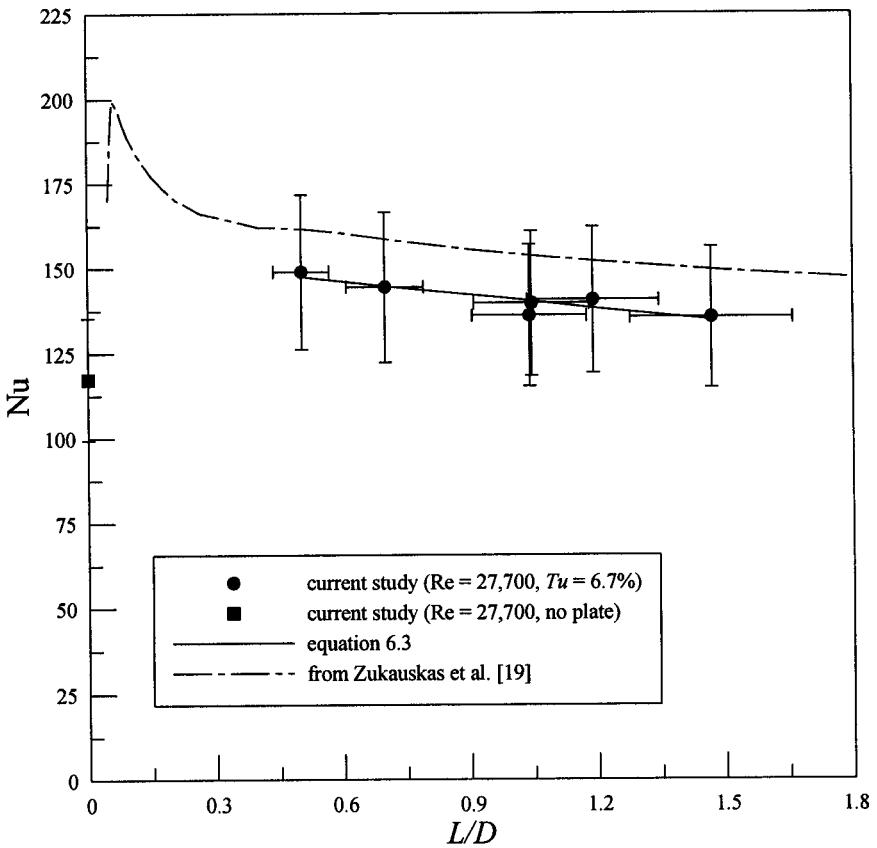

Figure 6.3. Relationship between Nusselt number and turbulence length scale ratio for the case of constant Reynolds number (Re = 27,700) and constant turbulence intensity (Tu = 6.7%).

Some researchers found that the turbulence length scale experiences a critical or peak region of heat transfer, whereupon, the heat transfer rate will steadily decrease with increasing turbulence length scale [13, 17, 19, 20, 22]. This maximum heat transfer occurs for values of $(L/D)\ \mathrm{Re}^{1/2} = 10$. Substituting the Reynolds number used in the current study (Re = 27,700) into this relationship yields a turbulence length scale ratio of approximately $L/D = 0.06$. This would suggest that the heat transfer is at its maximum at $L/D = 0.06$, which is considerably lower than the range of values studied by the author.

A comparison of Zukauskas et al.'s [19] work is shown in Figure 6.3. As is clearly seen, the heat transfer initially increases with increasing turbulence length scale until a maximum heat transfer occurs at the aforementioned value of $L/D = 0.06$. Once this point of maximum heat transfer occurs, a steady decrease in the heat transfer is then experienced with increasing turbulence length scale. This suggests that if the case of

very low turbulence level ($Tu < 0.6\%$) approximates the case of $L/D = 0$ with $Tu = 6.7\%$ as indicated by the solid square in Figure 6.3, it may be concluded that a peak could exist in the current experiment in the range $0 < L/D < 0.50$. Further research covering this low L/D range is needed to verify this.

CHAPTER 7 – CONCLUSIONS AND RECOMMENDATIONS

7.1 Conclusions

It has been shown that the effect of increasing Reynolds number corresponds to an increase in heat transfer for a uniform surface temperature circular cylinder in a cross flow of air. An expression that correlates the Reynolds number over the range 18,000 to 34,000 for $Tu < 0.6\%$ with the overall average heat transfer from the circular cylinder has been determined as,

$$\mathrm{Nu} = 0.78\sqrt{\mathrm{Re}} - 3.49.$$

The effects that turbulence intensity with a constant turbulence length scale and turbulence length scale with a constant turbulence intensity have on the overall average heat transfer for Re = 27,700 have also been determined experimentally. It was found that over the range of conditions considered,

- Increasing the turbulence intensity, from 3.0 to 8.2% while holding the turbulence length scale constant at $L/D = 0.78$, produces an increase in heat transfer, where the correlation equation is,

$$\mathrm{Nu} = 114.2 + 465.9Tu.$$

- Decreasing the length scale of the free stream turbulence, from 0.50 to 1.47 while holding turbulence intensity constant at $Tu = 6.7\%$, produces an increase in the heat transfer rate according to the relation,

$$\mathrm{Nu} = 140.0(L/D)^{-0.09}.$$

7.2 Recommendations

Work for the future should include:

- Experiments where turbulence intensity is varied for different values of constant turbulence length scale. This would consist of varying the turbulence intensity for a constant turbulence length scale value other than $L/D = 0.78$.
- Experiments where turbulence length scale is varied for different values of constant turbulence intensity. This would consist of varying the turbulence length scale for a constant turbulence intensity value other than $Tu = 6.7\%$.
- Extending the range of turbulence length scale considered for the case of constant turbulence intensity to determine the value of turbulence length scale where and if a maximum value of heat transfer is experienced.
- Extending the range of Reynolds number in order to develop a more comprehensive set of results.
- Increase the number of data points for each scenario from six.
- Change test parameters of the experiment, such as, cylinder diameter, aspect ratio, hole diameter and solidity ratio of the perforated plates to validate non-dimensional relationships.

REFERENCES

[1] Sanitjai, S., and Goldstein, R.J., "Effect of free stream turbulence on local mass transfer from a circular cylinder," International Journal of Heat and Mass Transfer, 44 (2001) 2863-2875.

[2] Rao, B.K., "Heat transfer to non-Newtonian flows over a cylinder in cross flow," International Journal of Heat and Fluid Flow, 21 (2000) 693-700.

[3] Blevins, R.D., "Flow-Induced Vibration," 2nd Edition, New York, Van Nostrand Reinhold, 1990.

[4] Churchill, S.W., and Bernstein, M., "A correlating equation for forced convection from gases and liquid to a circular cylinder in crossflow," Journal of Heat Transfer, 99 (1977) 300-306.

[5] Incropera, F.P., and DeWitt, D.P., "Fundamentals of Heat and Mass Transfer," 4th Edition, New York, John Wiley & Sons, 1996.

[6] Smith, M.C., and Kuethe, A.M., "Effects of turbulence on laminar skin friction and heat transfer," The Physics of Fluids, 9 (1966) 2337-2344.

[7] Çengel, Y.A., "Heat Transfer: A Practical Approach," Boston, Massachusetts, McGraw-Hill, 1998.

[8] Kondjoyan, A., and Boisson, H.C., "Comparison of calculated and experimental heat transfer coefficients at the surface of circular cylinders placed in a turbulent cross-flow of air," Journal of Food Engineering, 34 (1997) 123-143.

[9] Kondjoyan A., and Daudin J.D., "Effects of free stream turbulence intensity on heat and mass transfers at the surface of a circular cylinder and an elliptical cylinder, axis ratio 4," International Journal of Heat and Mass Transfer, 38 (1995) 1735-1749.

[10] Kondjoyan A., and Daudin J.D., "Heat and mass transfer coefficients at the surface of elliptical cylinders placed in a turbulent air flow," Journal of Food Engineering, 20 (1993) 339-367.

[11] Mehendale, A.B., Han, J.C., and Ou, S., "Influence of high mainstream turbulence on leading edge heat transfer," Journal of Heat Transfer, 113 (1991) 843-850.

[12] Galloway, T.R., "Enhancement of stagnation flow heat and mass transfer through interactions of free stream turbulence," AIChE Journal, 19 (1973) 608-617.

[13] Van der Hegge Zijnen, B.G., "Heat transfer from horizontal cylinders to a turbulent airflow," Applied Scientific Research, 7A (1958) 205-223.

[14] Lowery, G.W., and Vachon, R.I., "The effect of turbulence on heat transfer from heated cylinders," International Journal of Heat and Mass Transfer, 18 (1975) 1229-1242.

[15] Barrett, M.J., and Hollingsworth, D.K., "On the correlation of heat transfer in turbulent boundary layers subjected to free stream turbulence," Proceedings of the 33rd National Heat Transfer Conference, Albuquerque, New Mexico, August 15-17, 1999.

[16] Tennekes, H., and Lumley, J.L., "A First Course in Turbulence," 2nd Edition, Cambridge, Massachusetts, MIT Press, 1999.

[17] Zukauskas, A., Vaitiekunas, P., and Ziugzda, J., "Heat transfer from cylinders in transverse flows of highly variable turbulence," Heat Transfer Research, 29 (1998) 522-526.

[18] Vaitiekunas, A., Zukauskas, A., and Ziugzda, J., "Predicting the effect of the free stream turbulence intensity and integral length scale on the skin friction of and heat transfer from a circular cylinder," Heat Transfer Research, 25 (1993) 604-614.

[19] Zukauskas, A., Vaitiekunas, P., and Ziugzda, J., "Analysis of influence of free stream turbulence intensity and integral length scale on skin friction and heat transfer of a circular cylinder," Experimental Heat Transfer, Fluid Mechanics and Thermodynamics (1993) 591-596.

[20] Gorla, R., and Nemeth, N., "Effects of free stream turbulence intensity and integral length scale on heat transfer from a circular cylinder in crossflow," Proceedings of the 7th International Heat Transfer Conference, Munchen, 3 (1982) 153-158.

[21] Sunden, B., "A theoretical investigation of the effect of freestream turbulence on skin friction and heat transfer for a bluff body," International Journal of Heat and Mass Transfer, 22 (1979) 1125-1135.

[22] Yardi, N.R., and Sukhatme, S.P., "Effects of turbulence intensity and integral length scale of a turbulent free stream on forced convection heat transfer from a circular cylinder in cross-flow," Proceedings of the 6th International Heat Transfer Conference, Toronto, Canada, 5 (1978) 347-352.

[23] Sikmanovic, S., Oka, S., and Kondar-Djurdjevic, S., "Influence of the structure of turbulent flow on heat transfer from a single cylinder in a cross flow," Proceedings of the 5th International Heat Transfer Conference, II (1974) 320-324.

[24] Van Fossen, G.J., Simoneau, R.J., and Ching, C.Y., "Influence of turbulence parameters, Reynolds number, and body shape on stagnation-region heat transfer," Journal of Heat Transfer, 117 (1995) 597-603.

[25] Hijikata, K., Yoshida, H., and Mori, Y., "Theoretical and experimental study of turbulence effects on heat transfer around the stagnation point of a cylinder," Ihid., 3 (1982) 165-170.

[26] Dyban, Y.P., Epik, E.Y., and Kozlova, L.G., "Heat transfer in the vicinity of the front stagnation point of a cylinder in transverse flow," Heat Transfer, Soviet Research, 7 (1975) 70-73.

[27] Torii, S., and Yang, W., "Effects of the length scale of free stream turbulence and cylinder size on local heat transfer in laminar separated flows," Experimental Heat Transfer, 6 (1993) 175-187.

[28] Liu, R., "A study of the turbulence generated behind a perforated plate in a wind tunnel," Master's Thesis, Department of Mechanical, Automotive & Materials Engineering, University of Windsor, Windsor, Ontario, 2002.

[29] De Silva, I. and Fernando, H., "Oscillating grids as a source of nearly isotropic turbulence," Physics of Fluids, 6 (1994) 2455-2464.

[30] OMEGA Engineering, Inc., "The Electric Heaters Handbook," 28 (1992).

[31] National Institute of Standards and Technology, http://www.nist.gov.

[32] Figliola, R.S., and Beasley, D.E., "Theory and design for mechanical measurements," New York, John Wiley and Sons, Inc., 1991.

[33] Kline, S.J., and McClintock, F.A., "Describing uncertainties in single sample experiments," Mechanical Engineering, 75 (1953) 3-8.

APPENDIX A – THERMOCOUPLE COMPARISON

Four standard thermocouples were researched [30] for the current study to determine which thermocouple would be able to combine the most accurate reading with the highest sensitivity. A brief description of each of the thermocouples researched is given below as follows.

Type J The Iron – Constantan (Copper-Nickel) thermocouple with a positive iron wire and a negative Constantan wire is recommended in an operating range of up to 870°C for the largest wire sizes. Smaller size wires should operate in correspondingly lower temperatures.

Type T The Copper – Constantan (Copper-Nickel) thermocouple, with a positive copper wire and a negative Constantan wire is recommended for an operating range of up to 400°C. They are suitable for applications where moisture is present.

Type K The Chromel (Nickel-Chromium) – Alumel thermocouple with a positive Chromel wire and a negative Alumel wire is recommended in an operating range of up to 1260°C for the largest wire sizes. Smaller wires should operate in correspondingly lower temperatures.

Type E The Chromel (Nickel-Chromium) – Constantan (Copper-Nickel) thermocouple may be used for temperatures up to 870°C. At sub-zero temperatures, the thermocouple is not subjected to corrosion. This thermocouple has the highest e-m-f output of any standard metallic thermocouple.

One of the more important features of a thermocouple is how sensitive it is. Knowing that the temperature measurement is obtained by converting a voltage reading into a temperature reading, the sensitivity is a major factor as to how accurate results will be. With information provided by the National Institute of Standards and Technology [31], a comparison of sensitivity for the four types of thermocouples were calculated and plotted in Figure A.1.

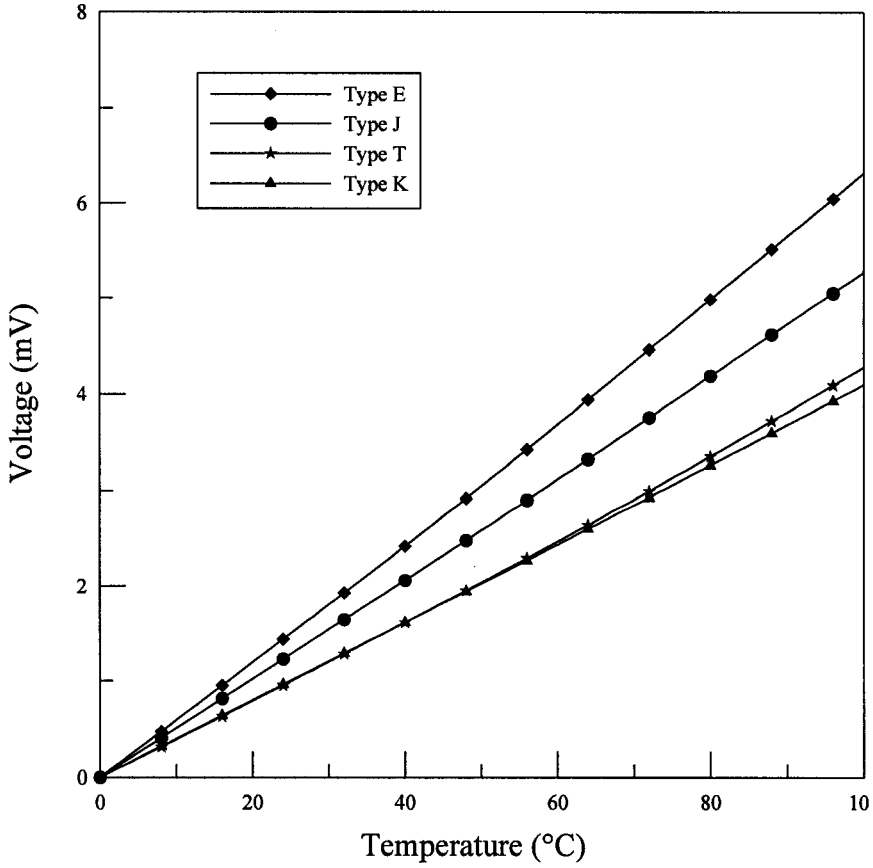

Figure A.1. Voltage change per change in temperature.

As illustrated, a Type E thermocouple has the greatest sensitivity because it has the steepest slope. In fact, the slope is approximately 1.5 times as great as a Type T and Type K thermocouple, and approximately 1.2 times as great as a Type J thermocouple.

Another factor that must be taken into consideration includes the accuracy of the thermocouple. Manufacturer standards indicate that even though a Type E thermocouple yields the highest voltage change per degree centigrade, it is not the most accurate. This distinction belongs to a Type T thermocouple, which from the data provided in Table A.1, has an accuracy of ± 1.0°C.

Table A.1. Sensitivity and accuracy of thermocouples researched.

Type	Sensitivity (mV/°C)	Accuracy (°C)
E	0.0621	± 1.7
J	0.0522	± 2.2
T	0.0418	± 1.0
K	0.0407	± 2.2

It is then concluded that because a Type E thermocouple is the most sensitive and a Type T thermocouple is the most accurate, a design-stage uncertainty analysis will be carried out. The following information for the thermocouple thermometer and each respective thermocouple has been gathered in order to determine which thermocouple will yield a measurement with the lowest uncertainty.

Thermocouple Thermometer

Resolution: 0.1°C

Accuracy: ± 0.1% of reading plus ± 0.4°C

Therefore the zero-order uncertainty is,

$w_0 = \pm 0.1°C$.

The instrument error (for a maximum temperature of 100°C) is,

$e_1 = (100°C \times 0.001) = 0.1°C$,

$e_2 = 0.4°C$,

$w_c = [e_1^2 + e_2^2]^{1/2} = \pm 0.412°C$.

Therefore a design-stage uncertainty is calculated to be,

$(w_d)_{\text{thermometer}} = [w_0^2 + w_c^2]^{1/2} = \pm 0.424°C$.

Type T Thermocouple

Accuracy: ± 1.0°C

Sensitivity: 0.0418 mV/°C

Resolution: 0.001 mV = (0.001 mV ÷ 0.0418 mV/°C) = 0.024°C

Therefore the zero-order uncertainty is,

$w_0 = \pm 0.024°C.$

The instrument error is,

$w_c = \pm 1.0°C.$

Therefore a design-stage uncertainty is calculated to be,

$(w_d)_{thermocouple} = [w_0^2 + w_c^2]^{½} = \pm 1.0003°C.$

Therefore the overall uncertainty for a Type T thermocouple is,

$w_d = [(w_d)^2_{thermometer} + (w_d)^2_{thermocouple}]^{½},$

$w_d = [(0.424°C)^2 + (1.0003°C)^2]^{½},$

$w_d = \pm 1.09°C.$

Type E Thermocouple

Accuracy: ± 1.7°C

Sensitivity: 0.0621 mV/°C

Resolution: 0.001 mV = (0.001 mV ÷ 0.0621 mV/°C) = 0.016°C

Therefore the zero-order uncertainty is,

$w_0 = \pm 0.016°C.$

The instrument error is,

$w_c = \pm 1.7°C.$

Therefore a design-stage uncertainty is calculated to be,

$(w_d)_{thermocouple} = [w_0^2 + w_c^2]^{½} = \pm 1.7001°C.$

Therefore the overall uncertainty for a Type E thermocouple is,

$w_d = [(w_d)^2_{thermometer} + (w_d)^2_{thermocouple}]^{½},$

$w_d = [(0.424°C)^2 + (1.7001°C)^2]^{½},$

$w_d = \pm 1.75°C.$

It is concluded that a Type T thermocouple (± 1.09°C) is more suited for the current application compared with a Type E thermocouple (± 1.75°C).

APPENDIX B – UNCERTAINTY ANALYSIS

Estimates of the uncertainty associated with the experiment were calculated by implementing a single-measurement uncertainty analysis as proposed by Figliola and Beasley [32]. These results were combined with the method of Kline and McClintock [33] to yield the ambiguity associated with all heat transfer and fluid flow related calculations.

Uncertainty Associated with Cylinder Diameter

Ten repeated measurements of cylinder diameter were made over time under fixed operating conditions (Table B.1). The diameter was measured using a digital caliper with the following instrument specifications:

Accuracy: ± 0.0254 mm = ± 0.0000254 m

Resolution: 0.01 mm = 0.00001 m

Therefore the uncertainty associated with instrument error is, $(w_c)_D = \pm 0.0000254$m. The zero-order uncertainty of the instrument is, $(w_0)_D = \pm 0.00001$m. The first-order uncertainty, or repeatability error, is $(w_1)_D = \pm t_{N\text{-}1,95} S_D$, where $t_{N\text{-}1,95} = t_{9,95} = 2.262$ and the standard deviation, $S_D = 0.0000344$ m. Thus $(w_1)_D = \pm 0.0000778$ m. Therefore the overall uncertainty associated with D is, $w_D = \pm [(w_c)_D^2 + (w_0)_D^2 + (w_1)_D^2]^{1/2} = \pm 0.0000825$ m.

Table B.1. Cylinder diameter data, $N = 10$.

n	1	2	3	4	5	6	7	8	9	10
D (mm)	50.83	50.89	50.88	50.82	50.84	50.82	50.90	50.81	50.89	50.87

Uncertainty Associated with Cylinder Length

The active length of the circular cylinder was designated as the region where the centre 'test' heater is embedded. This corresponds to the middle third region of the circular cylinder where the uncertainty is mostly due to the gap between the centre 'test'

heater and one of the adjoining guard heaters. This uncertainty was estimated to be half the distance of the gap. Therefore the uncertainty associated with ℓ is, $w_\ell = \pm 0.0048$ m.

Uncertainty Associated with Surface Area

The surface area was calculated as, $A_s = \pi D \ell$. Therefore the uncertainty associated with A_s is,

$$w_{A_s} = \sqrt{\left(\frac{\partial A_s}{\partial D} w_D\right)^2 + \left(\frac{\partial A_s}{\partial \ell} w_\ell\right)^2},$$

where, $\frac{\partial A_s}{\partial D} = \pi \ell$, and $w_D = \pm 0.0000825$ m,

$$\frac{\partial A_s}{\partial \ell} = \pi D, \text{ and } w_\ell = \pm 0.0048 \text{ m}.$$

Therefore $w_{A_s} = \pm 0.000767\,\text{m}^2$.

Uncertainty Associated with Emissivity

The emissivity of polished aluminium is $\varepsilon = 0.05$. The emissivity of rough aluminium is $\varepsilon = 0.07$. Therefore the uncertainty associated with ε is,

$$\begin{aligned} w_\varepsilon &= \pm\frac{1}{2}(\varepsilon_{\max} - \varepsilon_{\min}) \\ &= \pm\frac{1}{2}(0.07 - 0.05) \\ &= \pm 0.01. \end{aligned}$$

Uncertainty Associated with Surface Temperature

From Appendix A, the design-stage uncertainty of the surface temperature is calculated as, $(w_d)_{T_s} = \pm$ 1.09°C. The first-order uncertainty, due to the effect of time over the duration of a typical experiment, is calculated to be one-half the difference between $T_{s,\max}$ and $T_{s,\min}$, where $T_{s,\max}$ = 54.9°C and $T_{s,\min}$ = 51.8°C. Therefore $(w_1)_{T_s} = \pm$ 1.55°C. The average surface temperature found at each experimental condition is listed in Table B.2. From this information a second-order uncertainty, due to spatial variations, can be calculated as $(w_2)_{T_s} = \pm t_{N,95}\langle S_{T_s}\rangle$, where the pooled standard deviation, $\langle S_{T_s}\rangle$, is,

$$\langle S_{T_s}\rangle = \sqrt{\frac{1}{N}\sum_{n=1}^{N} S_{T_s}{}^2} \; .$$

Based on the data from Table B.2, $\langle S_{T_s}\rangle$ = 0.69°C. Therefore $(w_2)_{T_s} = \pm$ (2.101)(0.69°C) = ± 1.45°C. Thus the overall uncertainty associated with T_s is, $w_{T_s} = \pm [(w_d)_{T_s}{}^2 + (w_1)_{T_s}{}^2 + (w_2)_{T_s}{}^2]^{1/2} = \pm$ 2.39°C.

Table B.2. Surface temperature data, N = 18.

n	$\overline{T_s}$ (°C)	S_{T_s} (°C)	n	$\overline{T_s}$ (°C)	S_{T_s} (°C)	n	$\overline{T_s}$ (°C)	S_{T_s} (°C)
1	62.5	0.63	7	51.0	0.63	13	56.0	0.61
2	60.6	0.82	8	51.3	0.48	14	56.3	0.55
3	54.2	0.98	9	53.2	0.54	15	54.9	0.71
4	52.7	1.33	10	52.1	0.58	16	53.0	0.45
5	53.8	0.65	11	50.9	0.28	17	50.9	0.45
6	56.8	0.60	12	58.6	0.67	18	52.4	0.79

Uncertainty Associated with Free Stream Temperature

From Appendix A, the design-stage uncertainty of the surface temperature is calculated as, $(w_d)_{T_\infty} = \pm$ 1.09°C. The first-order uncertainty, due to the effect of time over the duration of a typical experiment, is calculated to be one-half the difference

between $T_{\infty,max}$ and $T_{\infty,min}$, where $T_{\infty,max}$ = 32.3°C and $T_{\infty,min}$ = 30.7°C. Therefore $(w_1)_{T_\infty}$ = ± 0.80°C. The overall uncertainty associated with T_∞ is, $w_{T_\infty} = \pm [(w_d)_{T_\infty}{}^2 + (w_1)_{T_\infty}{}^2]^{1/2}$ = ± 1.35°C.

Uncertainty Associated with the Heat Transfer Coefficient

The heat transfer coefficient was calculated as, $h = \dfrac{Q_{tot} - \varepsilon\sigma A_s\left(T_s^4 - T_\infty^4\right)}{A_s\left(T_s - T_\infty\right)}$.

Therefore the uncertainty associated with h is,

$$w_h = \sqrt{\left(\frac{\partial h}{\partial Q_{tot}} w_{Q_{tot}}\right)^2 + \left(\frac{\partial h}{\partial \varepsilon} w_\varepsilon\right)^2 + \left(\frac{\partial h}{\partial A_s} w_{A_s}\right)^2 + \left(\frac{\partial h}{\partial T_s} w_{T_s}\right)^2 + \left(\frac{\partial h}{\partial T_\infty} w_{T_\infty}\right)^2},$$

where, $\dfrac{\partial h}{\partial Q_{tot}} = \dfrac{1}{A_s\left(T_s - T_\infty\right)}$, and $w_{Q_{tot}} = \pm 2.5$ W $\left(\pm\frac{1}{2}\text{resolution}\right)$,

$$\frac{\partial h}{\partial \varepsilon} = -\frac{\sigma\left(T_s^4 - T_\infty^4\right)}{\left(T_s - T_\infty\right)}, \text{ and } w_\varepsilon = \pm 0.01,$$

$$\frac{\partial h}{\partial A_s} = -\frac{Q_{tot}}{A_s{}^2\left(T_s - T_\infty\right)}, \text{ and } w_{A_s} = \pm 0.000767\,\text{m}^2,$$

$$\frac{\partial h}{\partial T_s} = -\frac{Q_{tot}}{A_s\left(T_s - T_\infty\right)^2} - \varepsilon\sigma\left[\frac{4T_s^3}{\left(T_s - T_\infty\right)} - \frac{\left(T_s^4 - T_\infty^4\right)}{\left(T_s - T_\infty\right)^2}\right], \text{ and } w_{T_s} = \pm 2.39\,°\text{C},$$

$$\frac{\partial h}{\partial T_\infty} = \frac{Q_{tot}}{A_s\left(T_s - T_\infty\right)^2} - \varepsilon\sigma\left[-\frac{4T_\infty^3}{\left(T_s - T_\infty\right)} + \frac{\left(T_s^4 - T_\infty^4\right)}{\left(T_s - T_\infty\right)^2}\right], \text{ and } w_{T_\infty} = \pm 1.35\,°\text{C}.$$

Therefore $w_h = \pm$ 11.1 W/m^2 K.

Uncertainty Associated with the Thermal Conductivity of Air

The thermal conductivity at $T_{f,\max}$ = 0.0277 W/m K. The thermal conductivity at $T_{f,\min}$ = 0.0271 W/m K. Therefore the uncertainty associated with k_{air} is,

$$w_{k_{air}} = \pm\frac{1}{2}\left(k_{air,\max} - k_{air,\min}\right)$$
$$= \pm\frac{1}{2}\left(0.0277\,\text{W/m K} - 0.0271\,\text{W/m K}\right)$$
$$= \pm 0.0003\,\text{W/m K}.$$

Uncertainty Associated with Nusselt number

The Nusselt number was calculated as, $\text{Nu} = \frac{hD}{k_{air}}$. Therefore the uncertainty associated with Nu is,

$$w_{\text{Nu}} = \sqrt{\left(\frac{\partial \text{Nu}}{\partial h} w_h\right)^2 + \left(\frac{\partial \text{Nu}}{\partial D} w_D\right)^2 + \left(\frac{\partial \text{Nu}}{\partial k_{air}} w_{k_{air}}\right)^2},$$

where, $\frac{\partial \text{Nu}}{\partial h} = \frac{D}{k_{air}}$, and $w_h = \pm$ 11.1 W/m^2 K,

$$\frac{\partial \text{Nu}}{\partial D} = \frac{h}{k_{air}}, \text{ and } w_D = \pm\, 0.0000825 \text{ m},$$

$$\frac{\partial \text{Nu}}{\partial k_{air}} = -\frac{hD}{k_{air}^{\,2}}, \text{ and } w_{k_{air}} = \pm\, 0.0003 \text{ W/m K}.$$

Therefore $w_{\text{Nu}} = \pm$ 20.7.

Uncertainty Associated with the Density of Water

The density of water at $T_{f,\max}$ = 991.2 kg/m^3. The density of water at $T_{f,\min}$ = 988.6 kg/m^3. Therefore the uncertainty associated with ρ_{H_2O} is,

$$w_{\rho_{H_2O}} = \pm\frac{1}{2}\left(\rho_{H_2O,\max} - \rho_{H_2O,\min}\right)$$
$$= \pm\frac{1}{2}\left(991.2\,\text{kg/m}^3 - 988.6\,\text{kg/m}^3\right)$$
$$= \pm 1.3\,\text{kg/m}^3.$$

Uncertainty Associated with Room Temperature

An initial room temperature measurement was taken at the beginning of each experiment using the thermocouple located in the wind tunnel. The measurements are listed in Table B.3. From Appendix A, the design-stage uncertainty of the room temperature is calculated as, $(w_d)_{T_r}$ = ± 1.09°C. The first-order uncertainty, due to the effect of time, is $(w_1)_{T_r} = \pm\, t_{N\text{-}1,95}\, S_{T_r}$, where $t_{N\text{-}1,95} = t_{17,95}$ = 2.110 and the standard deviation, S_{T_r} = 1.65°C. Thus $(w_1)_{T_r}$ = ± 3.48°C. Therefore the overall uncertainty associated with T_r is, $w_{T_r} = \pm\,[(w_d)_{T_r}{}^2 + (w_1)_{T_r}{}^2]^{1/2} = \pm$ 3.65°C.

Table B.3. Room temperature data, N = 18.

n	1	2	3	4	5	6	7	8	9
T_r (°C)	28.4	27.2	24.7	24.4	24.6	25.2	25.1	23.2	24.2
n	10	11	12	13	14	15	16	17	18
T_r (°C)	23.2	23.2	23.5	27.7	27.1	26.4	24.5	23.6	24.1

Uncertainty Associated with Pressure

The uncertainty associated with pressure is calculated to be one-half the difference between $P_{\max}$ and $P_{\min}$, where $P_{\max}$ = 102,600 Pa and $P_{\min}$ = 101,030 Pa. Therefore w_P = ± 785 Pa.

Uncertainty Associated with the Density of Air

The density of air was calculated as, $\rho_{air} = \frac{P}{RT_r}$. Therefore the uncertainty associated with ρ_{air} is,

$$w_{\rho_{air}} = \sqrt{\left(\frac{\partial \rho_{air}}{\partial P} w_P\right)^2 + \left(\frac{\partial \rho_{air}}{\partial T_r} w_{T_r}\right)^2},$$

where, $\frac{\partial \rho_{air}}{\partial P} = \frac{1}{RT_r}$, and $w_P = \pm 785$ Pa,

$$\frac{\partial \rho_{air}}{\partial T_r} = -\frac{P}{RT_r^2}, \text{ and } w_{T_r} = \pm 3.65\,°\text{C}.$$

Therefore $w_{\rho_{air}} = \pm 0.017\,\text{kg/m}^3$.

Uncertainty Associated with Mean Velocity

The mean velocity in the wind tunnel was calculated using a manometer. The change in pressure is related to velocity in the following manner,

$$\overline{U} = \sqrt{\frac{2}{\rho_{air}} \Delta P},$$

where, $\Delta P = (\gamma_{oil})(0.1\ell_{oil})$
$= (0.827\gamma_{H_2O})(0.1\ell_{oil})$
$= (0.827\rho_{H_2O}g)(0.1\ell_{oil})$.

Therefore $\overline{U} = \sqrt{\frac{2}{\rho_{air}}(0.827\rho_{H_2O}g)(0.1\ell_{oil})} = \sqrt{0.1654g(\ell_{oil})\frac{\rho_{H_2O}}{\rho_{air}}}$.

Therefore the uncertainty associated with $\overline{U}$ is,

$$w_{\overline{U}} = \sqrt{\left(\frac{\partial\overline{U}}{\partial\ell_{oil}}w_{\ell_{oil}}\right)^2 + \left(\frac{\partial\overline{U}}{\partial\rho_{H_2O}}w_{\rho_{H_2O}}\right)^2 + \left(\frac{\partial\overline{U}}{\partial\rho_{air}}w_{\rho_{air}}\right)^2},$$

where, $\frac{\partial\overline{U}}{\partial\ell_{oil}} = 0.0827g\frac{\rho_{H_2O}}{\rho_{air}}\sqrt{\frac{1}{0.1654g(\ell_{oil})}\frac{\rho_{air}}{\rho_{H_2O}}}$, and

$w_{\ell_{oil}} = \pm 0.0005$ m $(\pm\frac{1}{2}$ resolution),

$\frac{\partial\overline{U}}{\partial\rho_{H_2O}} = 0.0827g\frac{\ell_{oil}}{\rho_{air}}\sqrt{\frac{1}{0.1654g(\ell_{oil})}\frac{\rho_{air}}{\rho_{H_2O}}}$, and $w_{\rho_{H_2O}} = \pm 1.3\,\text{kg/m}^3$,

$\frac{\partial\overline{U}}{\partial\rho_{air}} = -0.0827g\frac{(\ell_{oil})\rho_{H_2O}}{\rho_{air}^{\,2}}\sqrt{\frac{1}{0.1654g(\ell_{oil})}\frac{\rho_{air}}{\rho_{H_2O}}}$, and

$w_{\rho_{air}} = \pm 0.017\,\text{kg/m}^3$.

Therefore $w_{\overline{U}} = \pm 0.61$ m/s.

Uncertainty Associated with Dynamic Viscosity of Air

The dynamic viscosity of air at $T_{f,\max}$ = 0.0000195 kg/m s. The dynamic viscosity of air at $T_{f,\min}$ = 0.0000192 kg/m s. Therefore the uncertainty associated with μ is,

$$w_\mu = \pm\frac{1}{2}(\mu_{max} - \mu_{min})$$
$$= \pm\frac{1}{2}(0.0000195\,\text{kg/m s} - 0.0000192\,\text{kg/m s})$$
$$= \pm 0.00000015\,\text{kg/m s}.$$

Uncertainty Associated with Reynolds number

The Reynolds number was calculated as, $\text{Re} = \frac{\overline{U}D}{\nu} = \frac{\overline{U}D\rho_{air}}{\mu}$. Therefore the uncertainty associated with Re is,

$$w_{Nu} = \sqrt{\left(\frac{\partial \text{Re}}{\partial \overline{U}} w_{\overline{U}}\right)^2 + \left(\frac{\partial \text{Re}}{\partial D} w_D\right)^2 + \left(\frac{\partial \text{Re}}{\partial \rho_{air}} w_{\rho_{air}}\right)^2 + \left(\frac{\partial \text{Re}}{\partial \mu} w_\mu\right)^2},$$

where, $\frac{\partial \text{Re}}{\partial \overline{U}} = \frac{D\rho_{air}}{\mu}$, and $w_{\overline{U}} = \pm 0.61\,\text{m/s}$,

$$\frac{\partial \text{Re}}{\partial D} = \frac{\overline{U}\rho_{air}}{\mu}, \text{ and } w_D = \pm\, 0.0000825\ \text{m},$$

$$\frac{\partial \text{Re}}{\partial \rho_{air}} = \frac{\overline{U}D}{\mu}, \text{ and } w_{\rho_{air}} = \pm 0.017\,\text{kg/m}^3,$$

$$\frac{\partial \text{Re}}{\partial \mu} = -\frac{\overline{U}D\rho_{air}}{\mu^2}, \text{ and } w_\mu = \pm 0.00000015\,\text{kg/m s}.$$

Therefore $w_{\text{Re}} = \pm\, 1847.$

VITA AUCTORIS

Christopher Sak was born in 1977 in Windsor, Ontario, Canada. After attending St. Angela Elementary School, he graduated from Catholic Central High School in 1996. From there he went on to the University of Windsor where he obtained his Bachelor of Applied Science in Mechanical Engineering in 2000. He is currently a candidate for the Degree of Master of Applied Science in Mechanical Engineering at the University of Windsor.